J Solid State Electrochem (2011) 15:1049–1056
DOI 10.1007/s10008-010-1133-6

ORIGINAL PAPER

Gold nanoparticles electrooxidation: comparison of theory and experiment

Kh. Z. Brainina · Leonid G. Galperin · Ekaterina V. Vikulova · Natalia Yu. Stozhko · Aidar M. Murzakaev · Olga R. Timoshenkova · Yuri A. Kotov

Received: 29 April 2010 / Revised: 16 June 2010 / Accepted: 17 June 2010 / Published online: 6 July 2010

Abstract The article presents the findings of microscopic and electrochemical studies of size-dependent gold particles electrooxidation. Gold particles were immobilized on the surface of carbon-containing screen-printed electrodes. The experiment demonstrated that the transition from macroparticles to nanoparticles caused a shift of the maximum current potential of gold oxidation into the area with more negative potentials. A decrease in particle size resulted in an increase in the electrochemical activity of metal. A positive correlation between experimental and calculated curves confirms a mathematical model (2) and correctness of the calculations. Measured parameters of voltammograms, in particular, maximum current potential, can be used to describe the electrochemical activity and energy properties of nanoparticles.

Keywords Gold · Nanoparticles · Size effect · Electrochemical oxidation · Electron microscopy

K. Z. Brainina (✉) · E. V. Vikulova · N. Y. Stozhko
Ural State University of Economics,
8 Marta St, 62,
Ekaterinburg 620144, Russia
e-mail: baz@usue.ru

L. G. Galperin
Ural Federal University,
Mira St 19, A-203,
Ekaterinburg 620002, Russia

A. M. Murzakaev · O. R. Timoshenkova · Y. A. Kotov
Institute of Electrophysics,
Ural Branch of the Russian Academy of Science,
Amundsen St, 106,
Ekaterinburg 620016, Russia

Introduction

Physical properties of nanostructural materials differ significantly from macrosystems, particularly if we consider the effect of the metal particle radius on the melting point, surface tension, and optical properties (maximum absorption of colored metal sols) as well as catalytic and electrochemical ones [1, 5, 6, 8, 9, 11]. The prospect of using nanoparticles as sensors has aroused interest in a mathematical modeling of various processes [7, 8, 12], which clears the way for a quantitative analysis of particle properties. In contrast to previous proposed models based on purely geometric factors (particle shapes, particle distribution, and diffusion zones), Brainina et al. [2] have introduced thermodynamic considerations which take into account the energy characteristics of nanoparticles.

The goals of this study are to determine the size and energy effects on experimental voltammograms of gold nanoparticles electrooxidation, to compare the calculated voltammograms with the experimental ones, to justify the use of voltammograms as a source of information for the analysis of nanoparticle properties, and to study the electrochemical properties of gold nanoparticles with regard to a degree of their dispersion and distribution on the surface of a supporting electrode which has no effect other than to make an electrical contact at the nanoparticles and at which no electrolysis occurs at the potentials of interest.

Experimental section

Materials, instruments, and methods

The following chemically pure reagents were used: sodium citrate (Na-cit), hydrogen tetrachloroaurate (III) thrihydrate

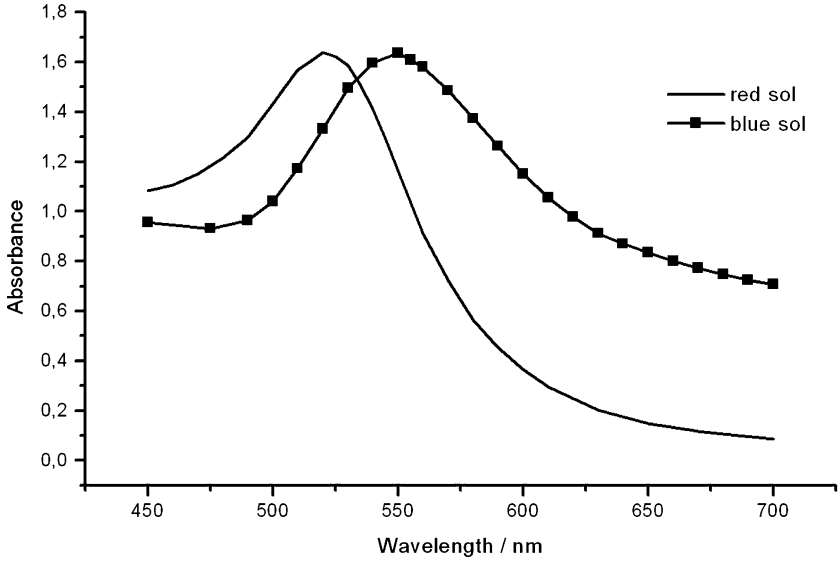

Fig. 1 Optical absorbance spectra for red and blue gold sols

($HAuCl_4 \times 3H_2O$), and acids (HCl, HNO_3). All solutions were prepared using deionized water with a resistivity of no less than 18 MΩcm, obtained with the membrane system DVS-M/1NA (18)-N (Russia).

Gold nanoparticles were synthesized by using a magnetic stirrer with heating IKA RCT basic (Germany).

UV–vis absorbance measurements were performed using a KFK-3 spectrophotometer (Russia) in the wavelength range of 400–700 nm with a 10-nm step. Particle size distribution in the sol and ξ-potential were determined by dynamic light scattering (DLS) with "Brookhaven ZetaPlus" universal suspension analyzer (USA). Transmission electron microscopy (TEM) imaging of colloidal gold nanoparticles was performed on a JEM-2100 transmission electron microscope (Japan) with LaB_6 cathode operating at an accelerating voltage of 200 kV (point resolution of 0.19 nm, line resolution of 0.14 nm). Before the microscopic examination, gold sols were kept in an ultrasonic field with the capacity of 300 W for 1–2 min generated by VCX 750 ultrasonic processor (USA). Then, a drop of suspension was placed onto an amorphous carbon film 5–6-nm thick and located on a standard copper grid of TEM. Scanning electron microscopy (SEM) imaging of gold particles on the surface of electrodes was performed on LEO 982 scanning electron microscope (Germany). The micrographs of the surface of the gold macroelectrode were performed by an optical microscope MIM-8 (Russia).

The electrochemical behavior of gold particles of different sizes was examined with potentiodynamic voltammetry by using IVA-5 (Russia), a semiautomatic inverse voltammetric analyzer interfaced to a personal computer and a three-electrode electrochemical cell. A glassy carbon rod was used as an auxiliary electrode; a saturated silver/silver chloride electrode (SCE) (E=0.22 V vs NHE) as a reference electrode. Modified and unmodified electrodes made of carbon- or gold-containing materials with the working surface area of 0.10 cm^2 were used as working electrodes.

Anodic voltammograms of gold were recorded at a linear potential sweep in the range from 0.5 to 1.4 V using 0.1 M HCl as the background electrolyte. The peak of gold oxidation potential (E, V), the maximum current (I, μA), and the quantity of electricity (Q, μC), which corresponded to the quantity of substance participating in the electrochemical process, were measured. Q was determined by graphical integration of the area under the anodic voltammograms of gold oxidation. All potentials are given relative to SCE.

Results and discussion

Preparation of the electrodes

A gold-'sputtered' (hereinafter 'bulk') electrode and thick-film carbon electrodes (TCE), ex situ modified with gold nanoparticles, were used as working electrodes. The bulk gold electrode was produced by vacuum metal sputtering from the wire surface (d=0.2 mm, 99.99% pure gold) onto

Table 1 Particle size and ζ-potential of gold sols

Sample	Average radius (weight distribution), nm	Prevailing size radius, nm; % of total quantity	ζ-potential, mV
Red sol	7.0	7.0–8.5 (100%)	−43.63±2.06
Blue sol	96.5	152.3–163.2 (~ 39%)	−47.88±1.62

polyethyleneterephthalate strip by VUP-4. The deposited gold layer was 0.5–1.0 mm thick.

Gold particles were immobilized on the surface of TCE. A few microliters of sol were placed on the surface of the electrode and left at room temperature in open air until completely dry. Cementit 3172 glue was applied to isolate the working area of the electrodes.

Synthesis of gold nanoparticles

Gold nanoparticles were synthesized by chemical reduction of aqueous solution of $HAuCl_4$ with sodium citrate in accordance with the accepted standard method [3]. Before the synthesis, all the glassware was kept in the mixture of three parts of HCl and one part of HNO_3 for an hour and then thoroughly rinsed with deionized water. Freshly prepared cit-Na solution was added to the boiling solution of 1×10^{-3} M $HAuCl_4$ under vigorous magnetic stirring (1,200 rpm) and boiled for another 15 min until full reduction of gold ions, as judged by ceased sol discoloration. Then, the sol was cooled to room temperature. Citrate ions acted both as a reducing agent and a stabilizer of gold nanoparticles; therefore, their concentration affected both the rate of reduction and the particle growth. In addition, the reaction led to the formation of oxidation products of citrate anions: 1.3-acetonedicarbon and itaconic acids which adsorbed on the particle surface and affected the particle growth [3]. In this regard, Au-NPs of different sizes were prepared by varying the ratio of $C(HAuCl_4)$:C(Na-cit). Smaller particles were obtained with the 1:5 ratio, whereas larger particles were obtained with the 1:1 ratio. In the first case, the sol of deep red was formed in the transmitted light ("the red sol"); in the second case, the sol was blue ("the blue sol"). Gold hydrosols with varying concentrations were prepared by diluting either the initial solution of $HAuCl_4$ or the concentrated sol. All synthesized sols were stored at +4°C in the dark.

Characterization of gold sol

In order to establish the characteristics of colloidal gold nanoparticles, UV–vis spectroscopy, DLS, and TEM were used.

UV–vis spectroscopy In the optical absorbance spectra of gold sols, a characteristic plasmon peak was observed

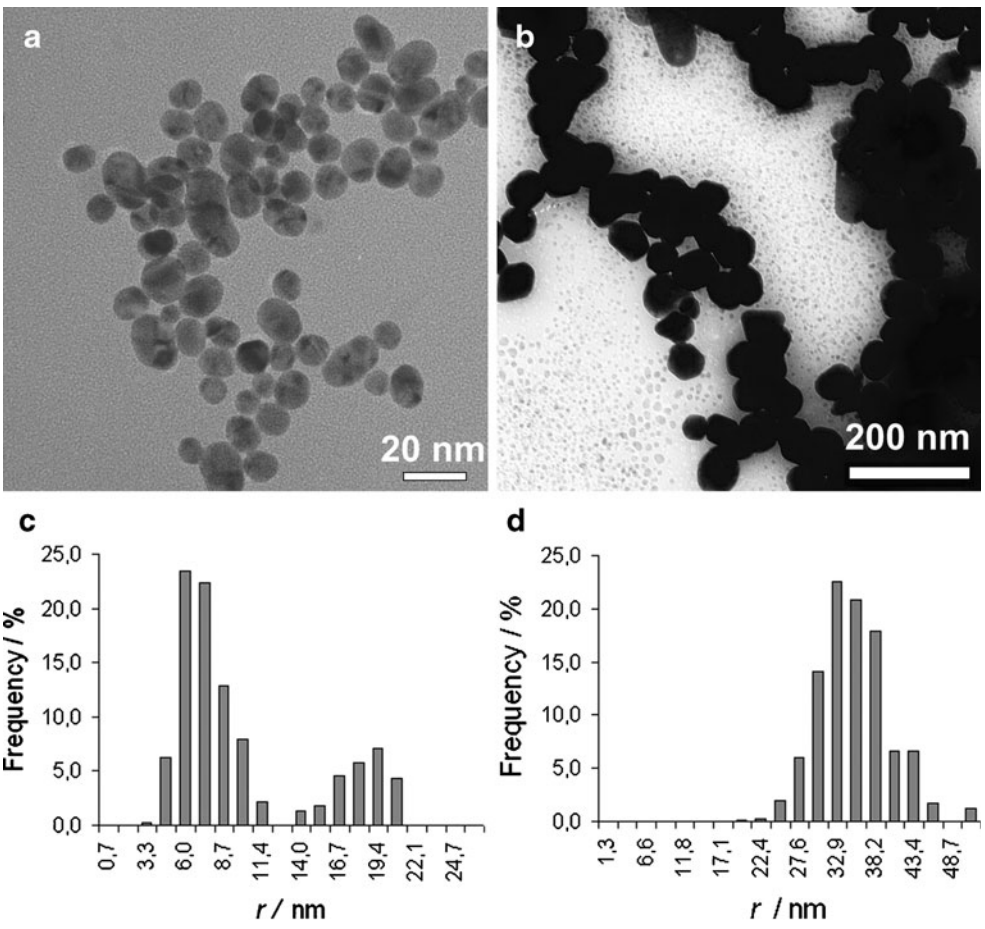

Fig. 2 TEM micrographs (**a**, **b**) and bar charts of varying size particle distribution (**c**, **d**) in the red gold sol (**a**, **c**) and in the blue gold sol (**b**, **d**)

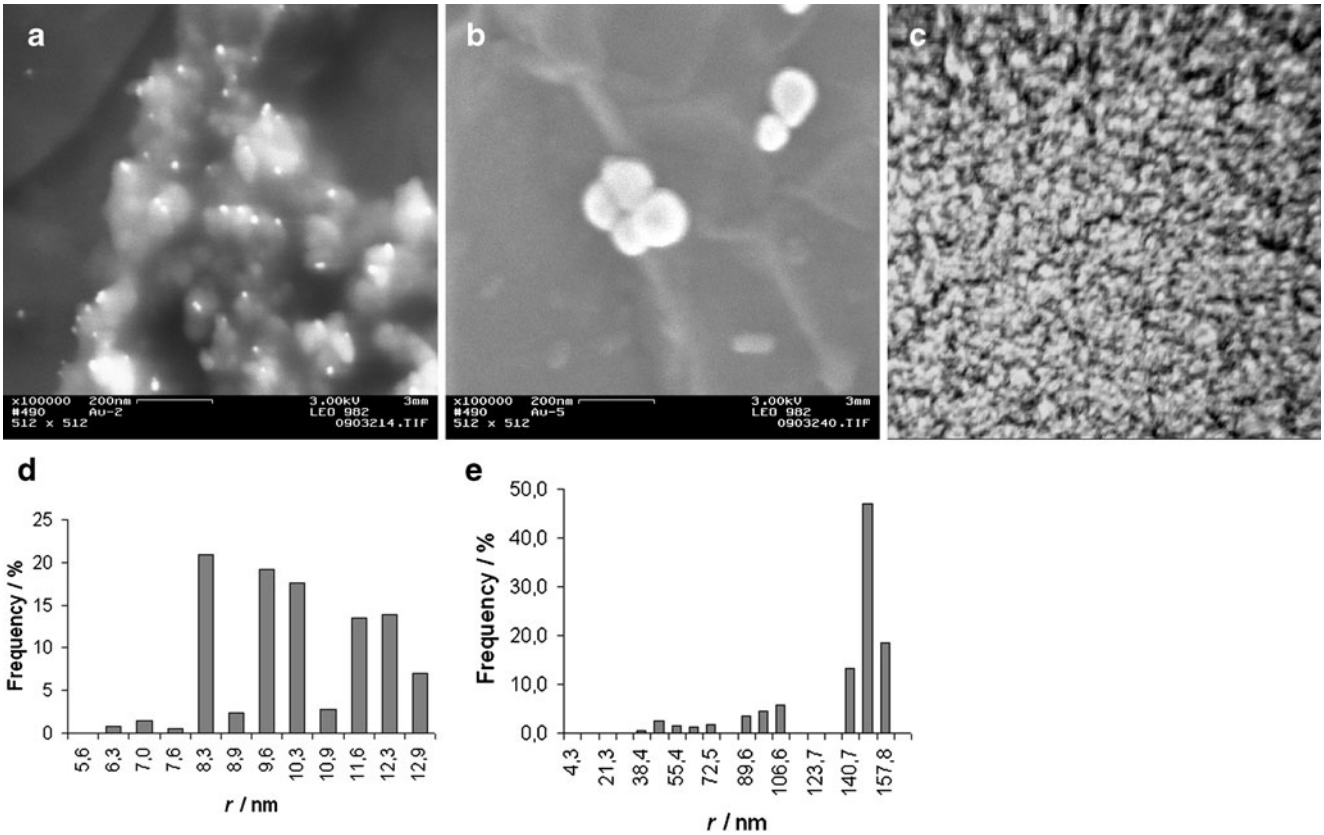

Fig. 3 SEM images of gold particles on TCE/Au_red (**a**) and on TCE/Au_blue (**b**); micrograph surface of bulk gold electrode (**c**); bar charts of varying particle size distribution on TCE/Au_red (**d**); TCE/Au_blue (**e**)

(Fig. 1), whose position was affected by the size and shape of nanoparticles in the sol and their local dielectric environment. An increase in the particle radius resulted in a shift of the peak wavelength (λ_{max}) to a longer wavelength [10]. In the optical absorbance spectrum of the red gold sol, the plasmon peak was observed at λ_{max}=520 nm (Fig. 1), which corresponded to the absorption of spherical gold nanoparticles with the radius of 10 nm [10]. In case of the blue sol, absorption maximum shifted to a longer wavelength (λ_{max} = 550 nm), which according to [4] was due to a larger radius (40 nm) of gold nanoparticles.

A broad shape of the plasmon peak of the blue sol, as compared with a peak of the optical density of the red sol, indicated a broader size distribution of gold nanoparticles.

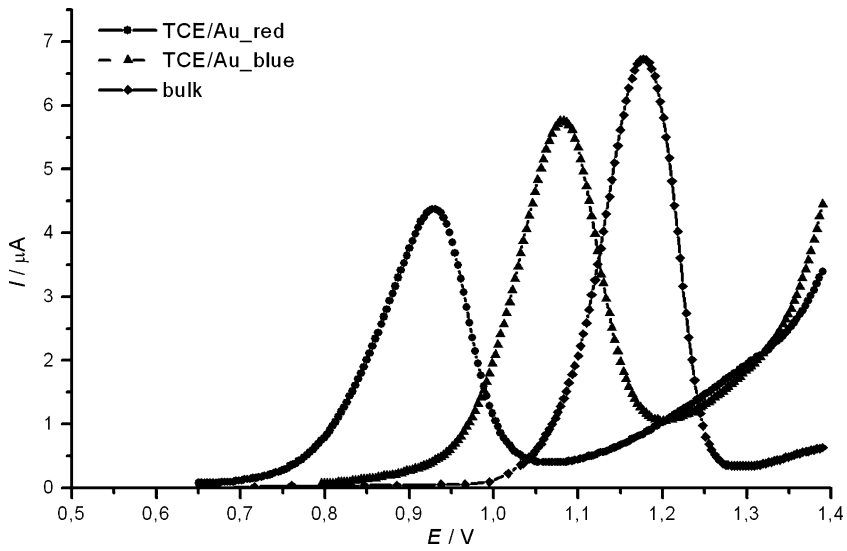

Fig. 4 Anodic voltammograms for TCE/Au_red (1), TCE/Au_blue (2), and bulk gold electrode (3). Background: 0.1 M HCl, υ=0.05 Vs^{-1}

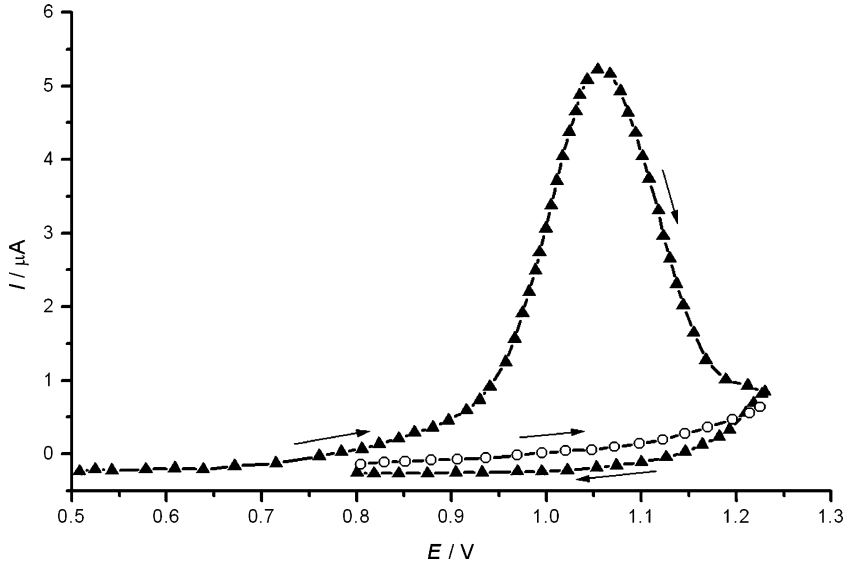

Fig. 5 Cyclic voltammogram (*triangle*) and second scan (*circle*) of TCE/Au_blue. Background: 0.1 M HCl, υ=0.05 Vs^{-1}. The *arrows* show the direction of the forward and reverse scan beginning at 0.5 V and ending at 1.23 V. The second scan beginning at 0.8 V and ending 1.23 V

DLS The study results of synthesized gold sols by DLS are shown in Table 1. The red sol demonstrated distinctive unimodal size distribution of particles, with the weighted average particle radius of 7.0 nm. In contrast, the blue sol was characterized by bimodal size distribution of particles, where the particles with the radius of 35.5–40.7 and 152.3–163.2 nm were represented almost equally. The particles with the radius of 152.3–163.2 nm are likely to be aggregates. The weighted average particle radius for the blue sol was 96.5 nm.

For both types of sols, a negative value of ζ-potential was typically ranging from −44 mV (the red sol) to −48 mV (the blue sol). This may result from the adsorption of citrate or chloride ions on the surface of the sols. The values of ζ-potential indicated that sol stability was affected mainly by electrostatic forces.

TEM Application of high-resolution TEM in the red and blue sols allowed to measure an average radius of gold nanoparticles at 6.5 and 33.1 nm, respectively (Fig. 2). Gold particles in synthesized sols generally had a shape closer to spherical. The blue sol was characterized by a broader size distribution. These data were consistent with the results obtained with DLS.

Characterization of gold particles on the electrode surface by SEM

Figure 3 shows SEM images of the surface of the TCE, modified with gold particles of different sizes and micrograph of the surface of the bulk gold electrode. The micrographs were performed by a scanning electron microscope (×100,000) and an optical microscope (×800), respectively.

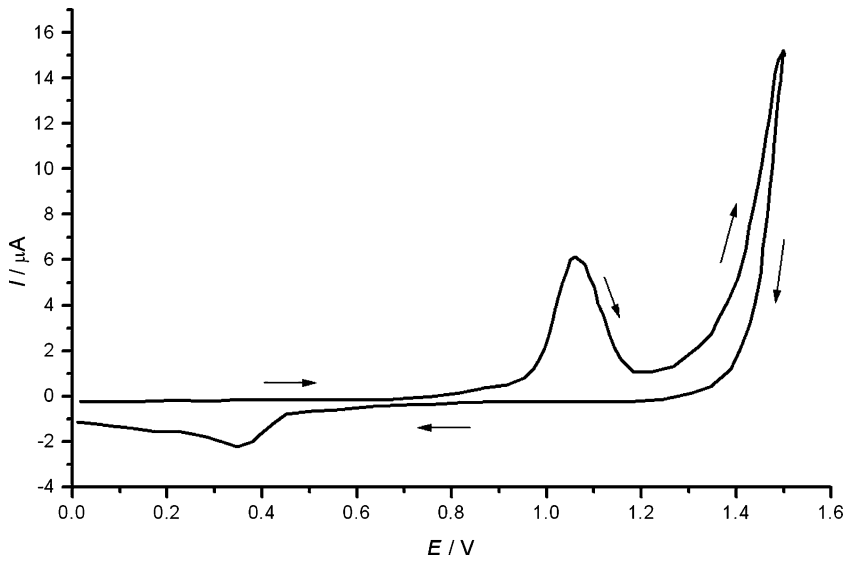

Fig. 6 Cyclic voltammogram of TCE/Au_blue. Background : 0.1 M HCl, υ=0.05 Vs^{-1}. The *arrows* show the direction of the forward and reverse scan beginning at 0 V and ending at 1.5 V

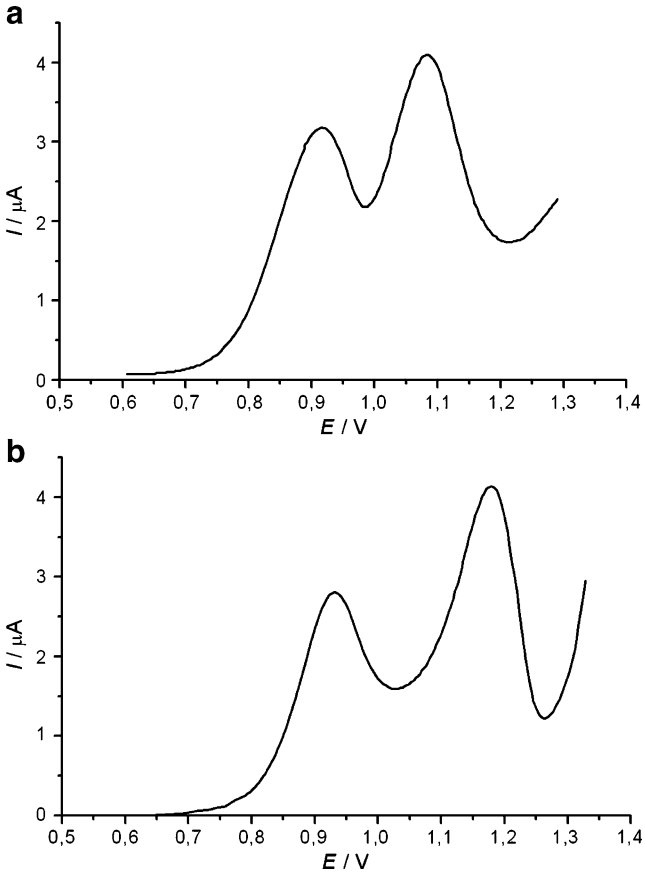

Fig. 7 Electrooxidation anodic voltammograms for 1:1 mixure of red and blue sols from the TCE (**a**) and the red sol from the bulk electrode (**b**). Background: 0.1 M HCl, v=0.05 Vs^{-1}

Gold particles immobilized on the surface of the TCE are shown as white spots mainly located on the elevated (gray) areas but virtually absent in the lower zones (black areas). Figure 3 shows that the surface morphology of the examined gold electrodes varies significantly. The radius of gold particles on the surface of the TCE, modified with the red sol (TCE/Au_red), ranges from 8.3 to 12.3 nm. Particles on the surface of TCE/Au_red are uniformly distributed. The distance between the particles exceeds their size three to 30 times. On the surface of the TCE, modified with the blue sol (TCE/Au_blue), single particles with a radius from 40 to 80 nm are observed as well as aggregates with a radius of 150 nm, consisting of two to four gold particles. An increase in the particle radius results in a smaller number of particles on the electrode surface. Thus, 1 μm^2 of TCE/Au_red may contain 30 particles on average, as compared to seven particles on 1 μm^2 of TCE/Au_ blue. Figure 3 also shows the size distribution of particles in the red and blue sols deposited on the electrode surface: in the red sol the majority particles have the radius of 10 nm, while in the blue sol the prevailing radius is 150 nm. Considering that electrochemical response is determined by the dominant particle size, these values were used for calculating gold oxidation voltammograms.

The surface of the bulk gold electrode has a granular structure. Taking into account the fact that the properties of the system consisting of particles with a radius equal to or exceeding 1 μm do not differ from the properties of the bulk phase [2, 6], the radius of the particles in the calculations is assumed to be 1 μm.

Electrochemical characteristic of gold particles of different sizes

The anodic voltammograms of gold, recorded in 0.1 M $HClO_4$, H_2SO_4, and HNO_3, all exhibit a broad peak which is unsuitable for evaluation. Apparently, the broad peak is caused by the formation of oxide (Au_2O_3) on the electrode surface. Electrochemical oxidation of gold from the surfaces of the bulk, TCE/Au_red, and TCE/Au_ blue

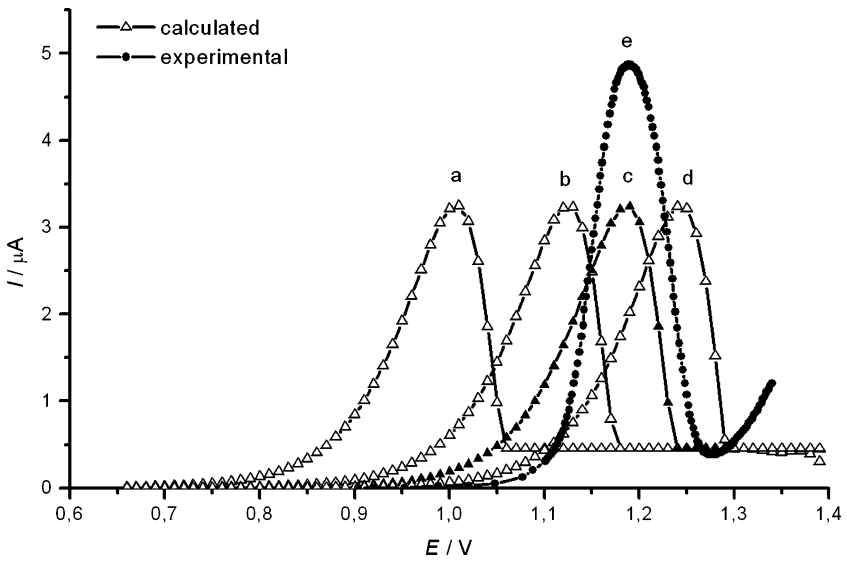

Fig. 8 Experimental and calculated voltammograms for bulk gold electrode electrooxidation. Background: 0.1 M HCl, v=0.05 Vs^{-1}. Calculation parameters: r =1 μm; Q=7.88 μC; $\Delta G°$=37 $Jmol^{-1}$, δ=1; k_s, 10^{-6} (**a**), 10^{-7} (**b**), 3×10^{-8} (**c**), 10^{-8} cm s^{-1} (**d**). Other parameters are given in Table 2

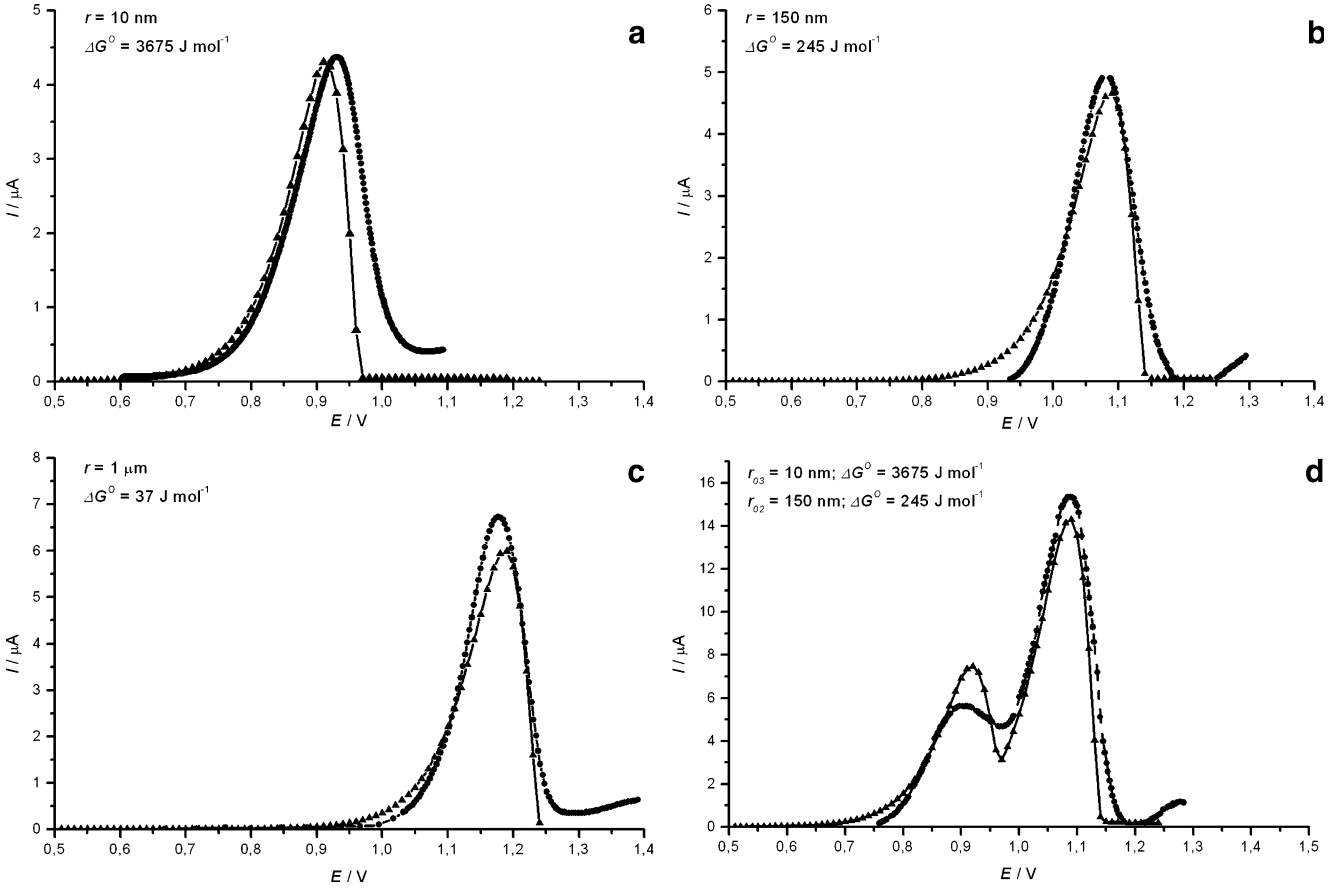

Fig. 9 Experimental (*circle*) and calculated (*triangular*) voltammograms of the gold particles electrooxidation. Background: 0.1 M HCl, v=0.05 Vs^{-1}. Calculation parameters: Q=10.07 μC, δ=1 (**a**); Q=11.30 μC, δ=1; (**c**) Q=14.57 μC, δ=1; (**b**); Q=49.42 μC, δ=0.3 (**d**). Other parameters are given in Table 2

electrodes in 0.1 M HCl was characterized by a clearly marked peak of oxidation current (Fig. 4). Figures 5 and 6 demonstrate that gold is removed from the surface of the electrode completely in one scan (there is no signal on the subsequent curve) and that the electrodissolution process is irreversible (big difference of anodic and cathodic peaks is observed). Experimental data showed an increasing electrochemical activity of gold particles due to smaller size effect. Transition from macro- to nanostructures resulted in a shift in the maximum gold oxidation current potential towards the cathodic potential region, which was observed on anodic voltammograms of gold.

The presence of particles of different sizes on the electrode surface caused the formation of a bifurcated signal (Fig. 7) whose shoulder height was affected by the mass concentration of particles of different sizes. Oxidation of particles of each size was observed in its own potential range. Thus, our experimental data agree with our previous theoretical propositions about electrooxidation of metal nanoparticles from the surface of the indifferent macroelectrode [2], where we took into account the energy differences between nano-, micro-, and macroparticles. For a quantitative analysis of data, numerical simulation of gold nanoparticles electrooxidation was done. The physical and mathematical model and calculations performed are presented in a previous paper [2]. The results of quantitative comparison of calculated and experimental data are presented in Figs. 8 and 9. In order to obtain a set of calculated gold electrooxidation voltammograms, we used

Table 2 Parameters used for calculating gold particles electrooxidation voltammograms

Parameter	Value
M, molar mass of gold	197 $gmol^{-1}$
ρ, density of gold	19.3 gcm^{-3}
σ, surface tension of gold on the boundary with air at 700°C	1,200 dyne cm^{-1}
n, number of electrons involved in the electrode process	1
δ, fraction of particles of a certain size	Relative unit
E_0, standard electrode potential of gold electrooxidation in $Au+Cl^- \rightarrow AuCl+e^-$	0.95 V
$\Delta G°$, Gibbs surface free energy	$Jmol^{-1}$

the parameters given in Table 2. All of them are tabulated values, except for the Gibbs free surface energy $\Delta G°$ and constant of the electrode process rate k_s. $\Delta G°$ was calculated as $\Delta G° = \sigma \times S$, where S is the total surface area of particles localized on the electrode surface. S was calculated with experimentally determined values of r and Q. In order to determine k_s, a set of voltammograms for the bulk electrode was calculated (Fig. 8). An agreement between the experimental and calculated curves was observed with $k_s = 3 \times 10^{-8}$ cm s^{-1}; thus, this value was taken for calculating gold nanoparticles electrooxidation voltammograms.

Figure 9 shows a comparison of the experimental and calculated voltammograms of electrooxidation for different-size gold particles. An agreement between the experimental and calculated curves confirms the choice of a relevant mathematical model and the correctness of the calculations, which allows to use signals of gold nanoparticles electrooxidation as a source of information about the size of metal particles and their electrochemical activity and energy state.

Conclusion

Presented in this work was a comparison of the experimental voltammograms of gold particles electrooxidation, and the voltammograms calculated with the mathematical model [2] allows the conclusion that measured parameters of voltammograms (I and E) can be used to describe some properties of nanosystems.

Thus, the earlier observed size effects are gradually transforming from qualitative empirical data into the data that can provide valuable information for analyzing the thermodynamic and energy properties of nanostructural materials, the kinetics of redox reactions of nanoparticles, which enables one to predict the properties of nanoparticles, in particular, the characteristics of modified nanoelectrode sensors.

Acknowledgments The authors express their deep gratitude to RFBR and the Government of Sverdlovsk Region for their financial support.

References

1. Abdullin TI, Bondar OV, Nikitina II, Bulatov ER, Morozov MV, Hilmutdinov AKh, Salakhov MKh, Culha M (2009) Bioelectrochemistry 77:37–42
2. Brainina KhZ, Galperin LG, Galperin AL (2010) J Solid State Electrochem 14:981
3. Chow MK, Zukoski CF (1994) J Colloid Interface Sci 165:97
4. Dhawan A, Muth JF (2006) Nanotechnology 17:2504
5. Inasaki T, Kobayashi S (2009) Electrochim Acta 54:4893
6. Jiang Q, Zhang S, Zhao M (2003) Mater Chem Phys 82:225
7. Jones SW, Cambell FW, Baron R, Xiao L, Compton RG (2008) J Phys Chem C 112:17820
8. Jones SW, Chevallier FG, Paddon CA, Compton RG (2007) Anal Chem 79:4110
9. Kalimuthu P, John A (2008) J Electroanal Chem 617:164
10. Liu X, Atwater M, Wang J, Huo Q (2007) Biointerfaces 58:3
11. Stozhko NYu, Malakhova NA, Bysov IV, Brainina KhZ (2009) J Anal Chem 64:1176
12. Streeter I, Baron R, Compton RG (2007) J Phys Chem C 111:17008